Pseudo-Critical Enhancement of Thermal Photons in Relativistic Heavy-Ion Collisions?

Hendrik van Hees[a,b], Min He[c], Ralf Rapp[d]

[a] *Frankfurt Institute for Advanced Studies, Ruth-Moufang-Straße 1, D-60438 Frankfurt, Germany*
[b] *Institute for Theoretical Physics, Max-von-Laue-Straße 1, D-60438 Frankfurt, Germany*
[c] *Department of Applied Physics, Nanjing University of Science and Technology, Nanjing 210094, China*
[d] *Cyclotron Institute and Department of Physics&Astronomy, Texas A&M University, College Station, TX 77843-3366, U.S.A.*

Abstract

We compute the spectra and elliptic flow of thermal photons emitted in ultrarelativistic heavy-ion collisions (URHICs) at RHIC and LHC. The thermal emission rates are taken from complete leading-order rates for the QGP and hadronic many-body calculations including baryons and antibaryons, as well as meson-exchange reactions (including Bremsstrahlung). We first update previous thermal fireball calculations by implementing a lattice-QCD based equation of state and extend them to compare to recent LHC data. We then scrutinize the space-time evolution of Au-Au collisions at RHIC by employing an ideal hydrodynamic model constrained by bulk- and multistrange-hadron spectra and elliptic flow, including a non-vanishing initial flow. We systematically compare the evolutions of temperature, radial flow, azimuthal anisotropy and four-volume, and exhibit the temperature profile of thermal photon radiation. Based on these insights, we put forward a scenario with a "pseudo-critical enhancement" of thermal emission rates, and investigate its impact on RHIC and LHC direct photon data.

Keywords: heavy-ion collisions, QCD phase diagram, direct photons
PACS: 25.75.-q, 25.75.Dw, 25.75.Nq

1. Introduction

The thermal emission rate of photons from strongly interacting matter encodes several interesting properties of the radiating medium (see, *e.g.*, Refs. [1, 2, 3, 4, 5] for reviews). Its spectral slope reflects the temperature of the system while its magnitude is related to the interaction strength of the charge carriers. In ultrarelativistic heavy-ion collisions (URHICs), the size of the interacting fireball is much smaller than the mean-free path of photons. Thus, the latter can probe the hot and dense interior of the medium. However, the observed photon spectra receive contributions from all reaction stages, *i.e.*, primordial NN collisions, pre-equilibrium, quark-gluon plasma (QGP) and hadronic phases, plus final-state decays of short-lived resonances (these so-called "direct" photons exclude decays of long-lived hadrons, *e.g.*, π and η). Calculations of direct-photon spectra require good control over both the microscopic emission rates and the space-time evolution of the medium. The latter not only determines the local emission temperature, but also

the collective-flow field which generally imparts a net blue-shift on the radiated photons. In addition, the azimuthal asymmetry of the thermal photon spectra, v_2^γ, is of interest [6, 7, 8, 9, 10, 11, 12, 13]: since the bulk v_2 requires several fm/c to build up, the observed value for photons helps to further constrain their emission history.

Direct-photon spectra in URHICs have been extracted in Pb-Pb($\sqrt{s} = 0.017\,A$TeV) collisions at the Super Proton Synchrotron (SPS) [14], in Au-Au($\sqrt{s} = 0.2\,A$TeV) at the Relativistic Heavy-Ion Collider (RHIC) [15], and in Pb-Pb($\sqrt{s} = 2.76\,A$TeV) at the Large Hadron Collider (LHC) [16]. At SPS, various theoretical models could approximately reproduce the measured spectra by adding thermal radiation from an equilibrated expanding fireball to a primordial component estimated from pp data [17, 18, 19, 20, 21]. The thermal yield prevailed over the primordial one up to transverse momenta of $q_T \approx$ 2-4 GeV. However, a decomposition into contributions from QGP and hadronic radiation, which would allow for a better characterization of the origin of the signal, remains ambiguous. By subtracting the primordial component from their data, the PHENIX Collaboration extracted the "excess radiation" and determined its inverse-slope parameter ("effective temperature") in Au-Au collisions at RHIC as $T_{\rm eff} = 221 \pm 19^{\rm stat} \pm 19^{\rm syst}$ MeV. Accounting for the aforementioned blue-shift effect, this result indicates that most of the radiation emanates from matter temperatures $T < 200$ MeV, challenging the notion of early QGP radiation [9]. A subsequent first measurement of the direct-photon v_2 supports this finding [22]: in the regime where thermal radiation is expected to be large, $q_T \lesssim 3$ GeV, $v_2^\gamma(q_T)$ turns out to be comparable to that of pions, which are only emitted at the end of the fireball evolution, *i.e.*, at thermal freezeout, $T_{\rm fo} \simeq 100$ MeV. The large v_2^γ, also found at LHC [23], thus puts rather stringent constraints on the origin of the excess photons.

In previous work [9] we have calculated thermal photon spectra at RHIC, differing from existing calculations in mainly two aspects. First, a more extensive set of hadronic thermal photon rates has been employed [19], which, in particular, includes the contributions from baryons and antibaryons (known to be important in the dilepton context [24, 25]). These rates approximately match complete leading-order (LO) QGP rates around the pseudo-critical temperature, $T_{\rm pc} \simeq 170$ MeV [26], thus rendering a near continuous emissivity across the transition region. Second, a schematic medium evolution was constructed utilizing a blast-wave type elliptic-fireball model, quantitatively fit to spectra and v_2 of bulk hadrons (π, K, p) at $T_{\rm fo} \simeq 100$ MeV and multistrange hadrons (e.g., ϕ and Ω^-) at $T_{\rm ch} = 170$ MeV. The implementation of this "sequential freezeout" is phenomenologically motivated [27], and, in particular, leads to a saturation of the bulk-medium v_2 close to the transition regime, after about 4-6 fm/c for central and semi-central Au-Au collisions at RHIC. As a result, the direct-photon v_2 increased by a factor of ~ 3 over existing calculations, reaching into the error bars of the PHENIX data.

In the present paper we expand on and scrutinize these findings by extending the calculations to LHC energy and then employing a previously constructed ideal hydrodynamic bulk-evolution [28] to conduct a detailed comparison to the emission characteristics of the fireball. Much like the latter, this hydro evolution has been quantitatively constrained by bulk-hadron spectra and v_2, utilizing the concept of sequential freezeout. Both evolutions will be based on a lattice-QCD equation of state (EoS) for the QGP, matched to a hadron resonance gas (HRG) with chemical freezeout. The comparisons will encompass the time evolution of radial and elliptic flow, temperature, four volume and photon emission profile. Motivated by these comparisons, which identify the transition

region as a key contributor to thermal photon spectra, we conjecture an enhancement of the currently available photon emission rates around $T_{\rm pc}$ and explore in how far this could help to resolve the discrepancies with the data.

Our article is organized as follows. In Sec. 2 we recall basic ingredients and features of the fireball (Sec. 2.1) and hydrodynamic (Sec. 2.2) bulk evolutions, including analyses of their time and temperature profiles of collective flow and four volume (Sec. 2.3). In Sec. 3 we investigate the spectra and elliptic flow of thermal photons emitted from the fireball (Sec. 3.1) and hydro (Sec. 3.2), and (after adding primordial production) compare to recent RHIC and LHC data. In Sec. 4 we analyze the differences in the fireball and hydro photon results in view of the insights from Sec. 2 and discuss possible origins of current discrepancies with data. We conclude and outline future investigations in Sec. 5.

2. Bulk Evolution Models

The calculation of thermal-photon spectra in URHICs is based on the differential emission rate per unit phase space from a strongly interacting medium of temperature T and baryon-chemical potential μ_B,

$$q_0 \frac{dN_\gamma}{d^4x d^3q} = -\frac{\alpha_{\rm EM}}{\pi^2}\, f^B(q_0;T) \times {\rm Im}\,\Pi^T_{\rm EM}(q_0=q;\mu_B,T)\ . \tag{1}$$

Here, the rate is written in terms of the 3-D transverse part of the electromagnetic current correlator, $\Pi^T_{\rm EM}$, and the thermal Bose distribution function, $f^{\rm B}$, where $q_0 = q$ denote the energy and three-momentum of the photon in the local rest frame of the medium. This expression is leading order in the electromagnetic (EM) coupling $\alpha_{\rm EM}$, required to produce the photon without further EM interaction when traversing the fireball. Alternatively, one may express the rate in terms of photon-production scattering matrix elements, appropriately convoluted over the thermal distribution functions of the incoming particles. This approach is usually more convenient when evaluating tree-level diagrams (*e.g.*, t-channel meson exchanges) which are expected to prevail at high photon energies [19].

The calculation of a thermal photon spectrum in URHICs requires to integrate the above rate over the entire four-volume of the reaction, $V_4 = \int {\rm d}^4x$, accounting for the local temperature and collective expansion velocity of the emission point. In the following, we will briefly recall how this four-volume integration is done in two different models, *i.e.*, a schematic blast-wave type fireball (Sec. 2.1) and ideal hydrodynamics (Sec. 2.2); both are based on the same equation of state and fits to the same set of bulk-hadron observables. This will be followed by a detailed comparison of the flow, temperature and four-volume profiles (Sec. 2.3).

2.1. Thermal Fireball

The thermal fireball model is based on an isotropically expanding cylinder with volume

$$V_{\rm FB}(t) = \pi a(t) b(t) (z_0 + ct), \tag{2}$$

where the elliptic transverse area is characterized by semi-major and semi-minor axes, $a(t)$ and $b(t)$, respectively. Their initial values are estimated from the nuclear overlap

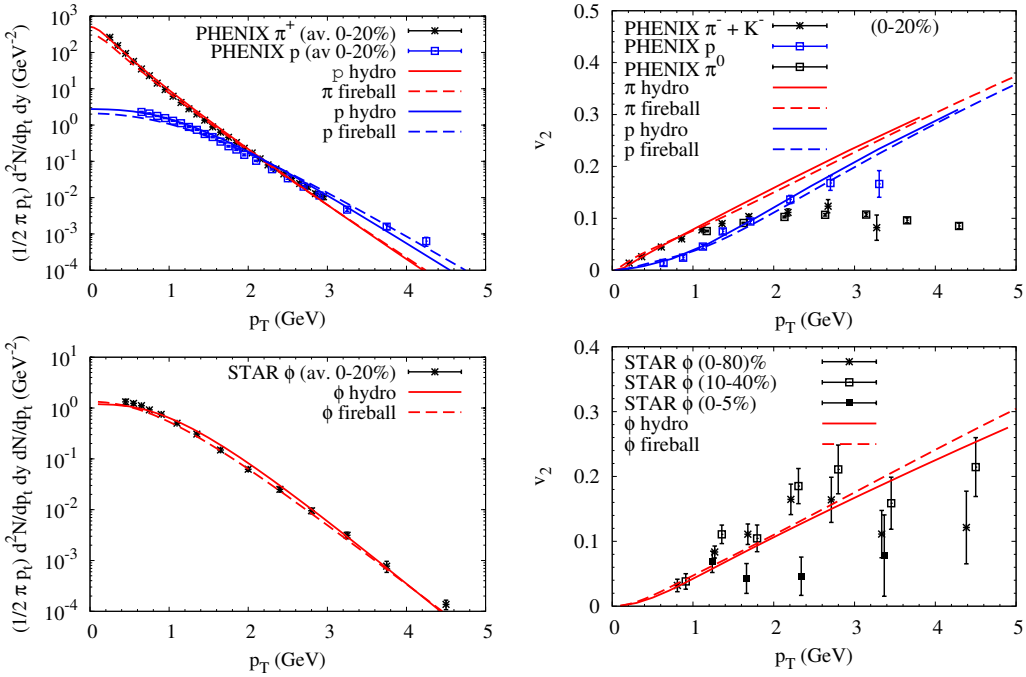

Figure 1: (Color online) Fits to the spectra and elliptic flow of light hadrons ($T_{\rm fo} \simeq 110\,$MeV, upper two panels) and ϕ mesons ($T_{\rm fo} = 160\,$MeV, lower two panels) in Au-Au($\sqrt{s} = 200\,A$GeV) collisions, using EoS *latPHG* within either the fireball (dashed lines) or ideal hydrodynamic model (solid lines). The data are taken from Refs. [33, 34, 35, 36].

at given impact parameter, while the initial longitudinal size, z_0, controls the formation time of the thermal medium. Assuming a constant total entropy, $S_{\rm tot}$, of the fireball at given collision centrality (fixed by the observed number of charged particles), the time evolution of the entropy density follows as $s(t) = S_{\rm tot}/V_{\rm FB}(t)$. Once the EoS is specified, i.e., the temperature dependence of s, one can convert $s(t)$ into $T(t)$. In our previous calculations of thermal-photon spectra [9] we used a quasi-particle QGP EoS with a first-order transition into a HRG and chemical freezeout at $T_{\rm c} = T_{\rm ch} = 180\,$MeV [24]. Here, we update the EoS with a fit to lattice-QCD data for the QGP part [28], smoothly matched to a HRG at $T_{\rm pc} = 170\,$MeV and chemical freezeout at $T_{\rm ch} = 160\,$MeV, at both RHIC and LHC energies [29, 30]. For $T < T_{\rm ch}$, effective chemical potentials for pions, kaons, antibaryons etc., are introduced [31] to preserve the finally observed hadron ratios extracted from the chemical-freezeout fits, while strong processes (*e.g.*, $\pi\pi \leftrightarrow \rho$) are assumed to maintain chemical equilibrium (so-called *partial* chemical equilibrium). Following Ref. [28] we refer to this EoS as "*latPHG*".

With this set-up, the time dependence of the elliptic radii, $a(t)$ and $b(t)$, can be constructed with guidance from hydrodynamic models [32] to approximately reproduce their time evolution of the radial and elliptic flow, as well as momentum-space anisotropy [9]. In addition, the idea of sequential freeze-out has been implemented, *i.e.*, a kinetic decoupling of multistrange hadrons (*e.g.*, ϕ and Ω^-) at chemical freezeout. This requires a somewhat faster transverse expansion than in the original hydro models [32], but is

consistent with the observed phenomenon of constituent-quark number scaling of elliptic flow. Importantly, it implies that the bulk-v_2 essentially saturates close to $T_c \simeq T_{ch}$. With a suitable choice in initial conditions this can be recovered in hydrodynamic simulations [28], as we will see below. For a more accurate reproduction of the final-state hadron multiplicities compared to our previous work [9] (accounting for the modified EoS, feeddown and a narrowing of the fireball rapidity distributions due to the large transverse flow), we have reduced the total entropy in our fireball by ca. 20%. With a freeze-out temperature of $T_{fo} \simeq 100(160)\,\mathrm{MeV}$, the measured p_T spectra and elliptic flow of light (multistrange) hadrons can be reasonably well described, cf. dashed lines in Fig. 1[1]. One might be concerned that the calculated $v_2(p_T)$ for thermal pions and protons exceeds the data toward higher p_T, in a regime which is still relevant for thermal photon production. However, the thermal p_T spectra start to underpredict the experimental yields data in this regime. For example, for pions with $p_T \simeq 3\,\mathrm{GeV}$, the thermal spectrum accounts for ca. 65% of the experimental yield; weighting the thermal pion-v_2 of $\sim 22\%$ with this fraction gives $\sim 14\%$, which is not far from the data, $v_2(p_T = 3\mathrm{GeV}) \simeq 11\%$. While these estimates pertain to kinetic freezeout, the calculations for the ϕ meson represent a snapshot at $T_{ch} = 160\,\mathrm{MeV}$; they approximately follow the measured spectra and v_2 out to higher p_T.

2.2. Ideal Hydrodynamics

The hydrodynamic model used in the present study has been described in detail in Ref. [28]. It is based on the 2+1-dimensional ideal hydro code of Ref. [32] (AZHYDRO), augmented with the updated EoS described above (*latPHG*) and initial conditions tuned to reproduce bulk and multistrange hadron yields, spectra and v_2 in central and semi-central Au-Au collisions at full RHIC energy. Specifically, a rather compact initial-entropy density profile was adopted, proportional to the binary-collision density in the optical Glauber model (this is not unlike what has been obtained in gluon saturation models); with a thermalization time of $\tau_0 = 0.6$ fm/c, the central initial temperature amounts to $T_0 = 398$ MeV in 0-20% Au-Au($\sqrt{s_{NN}} = 200$ GeV). Furthermore, a sizable initial radial flow with a surface value of around $0.13c$ has been introduced (and a very small positive v_2 to optimize the hadron fits). All of these features (lattice EoS, compact initial profile and initial radial flow) lead to a more violent radial expansion, which enables an improved description of the bulk-hadron v_2 at kinetic freezeout even within ideal hydrodynamics. At the same time, it generates an earlier saturation of the bulk-medium v_2, which, in particular, requires multistrange hadrons to freeze out at the chemical freezeout temperature T_{ch} to reproduce their p_T spectra and v_2 (this is not unwelcome as their hadronic cross sections might be too small to maintain kinetic equilibrium at lower temperatures). A more violent expansion has also been identified as a key to the solution of the "HBT puzzle" [37]. As emphasized in Ref. [28], the ideal-hydro tunes are not meant to supplant principally more realistic viscous evolutions, but rather to explore limitations and flexibilities in the (ideal-) hydro description, within "reasonable" variations of the input. In Fig. 1, the solid lines show some of the hydro results for bulk spectra and elliptic flow in comparison to RHIC data, which turn out to be very similar to the schematic fireball.

[1] We have not removed the entropy lost to multistrange hadrons (which amounts to ∼2%) from the fireball; we neglect this correction in both fireball and hydro evolution.

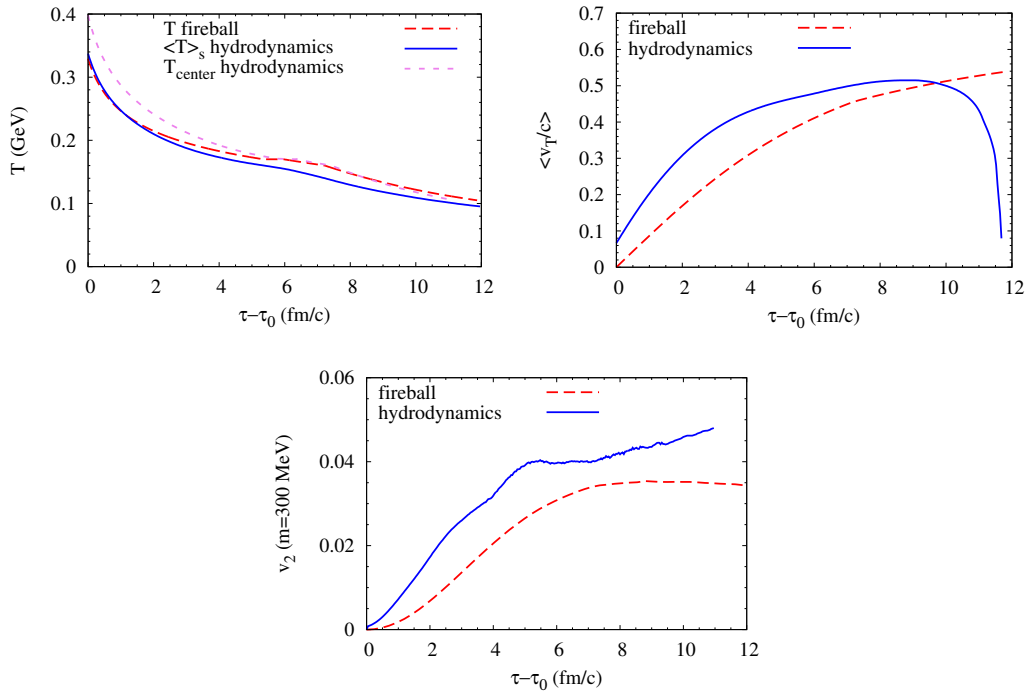

Figure 2: (Color online) Time evolution of average temperature (upper left panel), average transverse flow velocity (upper right panel) and elliptic flow (lower panel, using a particle mass of $m = 300\,\mathrm{MeV}$) in the expanding fireball (dashed lines) and hydrodynamic evolution (solid lines). In addition, the upper left panel contains the temperature evolution of the central hydro cell (short-dashed line).

2.3. Comparison of Space-Time Properties

We are now in position to systematically compare the space-time evolutions of the schematic fireball and the ideal hydro solution. We focus on 0-20% central Au-Au collisions at RHIC energy ($\sqrt{s} = 200\,A\mathrm{GeV}$), where both models describe the bulk spectra and v_2 fairly well, based on the same EoS (*latPHG*). Since the isotropic nature of the fireball is rather schematic compared to the more elaborate profiles in the hydro evolution, we investigate in this Section how this difference manifests itself in suitably averaged bulk quantities, which are expected to play an important role in the photon emission observables discussed in the next Section.

Let us first investigate the time evolution of (average) temperature, radial and elliptic flow, see Fig. 2. The temperature of the fireball is generally rather close to the average one from the hydro model, but exhibits systematically slightly higher values in the late states of the evolution (see upper left panel). This goes along with a 10-15% longer lifetime of the fireball evolution, indicating a somewhat slower cooling in the later stages. The radial flow (upper right panel of Fig. 2) starts out higher in the hydro (due to finite initial flow), but then levels off more quickly than in the fireball, eventually dropping below the latter's. For the elliptic flow comparison, we evaluate the v_2 coefficient of the momentum spectra of particles with an average mass of 300 MeV at fixed proper time (lower panel

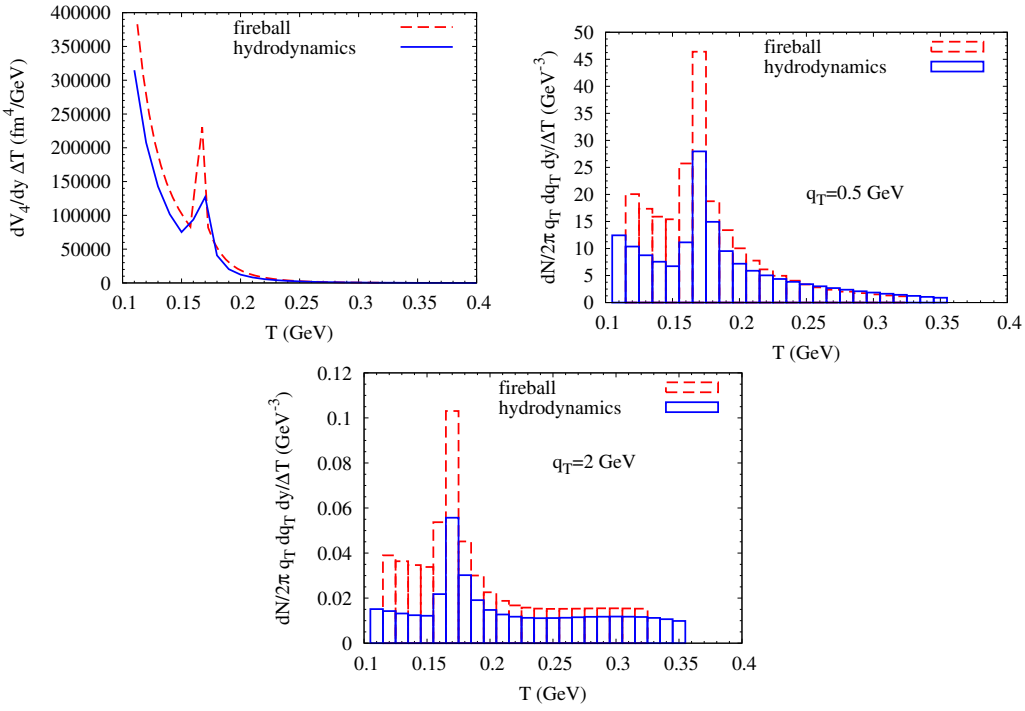

Figure 3: (Color online) Temperature evolution of the differential emission four-volume (upper left panel) and the double-differential photon emission rate (QGP for $T > T_{\rm pc}$ and hadronic for $T < T_{\rm pc}$) for two transverse momenta ($q_T = 0.5\,\mathrm{GeV}$ and $q_T = 2\,\mathrm{GeV}$ in the upper right and lower panel, respectively), in the expanding fireball (dashed lines) and hydrodynamic evolution (solid lines).

of Fig. 2). For the hydrodynamic evolution this involves a varying temperature while the fireball is spatially homogeneous at each time.

To properly interpret the observed photon spectra it is important to understand how the different emission stages contribute to the total. From the rate expression, Eq. (1), one sees that the weighting is governed by three ingredients: the (differential) four-volume, the thermal weight (Bose factor) and the EM spectral function (at the photon point). The former two are governed by the bulk-medium evolution. To make a closer connection to the underlying matter properties, we now plot pertinent quantities as a function of temperature, rather than time. The upper left panel in Fig. 3 shows the T dependence of the differential four-volume, $\Delta V_4/\Delta T$, over temperature intervals of $\Delta T = 10\,\mathrm{MeV}$ (and per unit rapidity). For both fireball and hydro evolution this quantity shows a distinct maximum structure around the pseudocritical temperature of $T_{\rm pc} \simeq 170\,\mathrm{MeV}$, as a consequence of the rapid change in the entropy density in the EoS (a remnant of the latent heat). One also finds a pronounced increase in the differential four-volume in the late(r) hadronic stages of the collision (stipulating the importance of a realistic hadronic photon emission rate). Again we find that the ideal hydro evolution seems to cool somewhat faster than the fireball (this might slightly change in a viscous

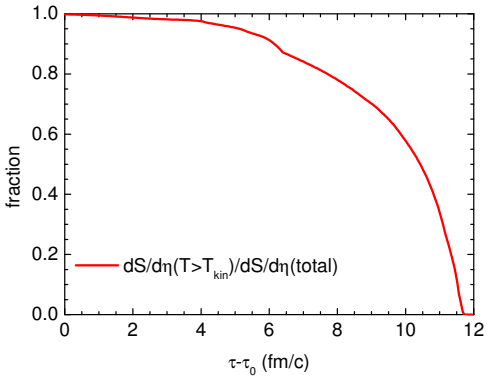

Figure 4: (Color online) Time evolution of the entropy fraction (relative to the total) which is in fluid cells at temperatures above the kinetic freezeout temperature in the hydrodynamic model.

evolution where some of the expansion work is dissipated into heat). Whereas hadron emission at kinetic freezeout in the hydro evolution is a continuous process, the fireball freezeout of the entire three-volume occurs at the end of the evolution. This difference is illustrated in Fig. 4, where we plot the *time* dependence of the fraction of the total entropy that is above the kinetic-freezeout temperature in the hydro evolution. This fraction shows a marked departure from one at times already well before the total lifetime; in contrast, this fraction is equal to one throughout the fireball evolution. Recall, however, that the three-volume at small temperatures must be very similar in both evolutions, since the total three-volume at freeze-out figures into the calculation of hadron multiplicities (and spectra), which agree rather well. Our hydro evolution, on the other hand, does not allow for the possibility that the freeze-out front "re-swallows" previously frozen-out matter cells. This effect has been studied, *e.g.*, in Ref. [38], where it was found to be significant even in the context of hadron observables. It would be interesting to investigate its impact on thermal-photon spectra.

The increase in emission four-volume is counteracted by the drop in temperature, suppressing the thermal distribution function in the rate. This renders the energy argument in the Bose function as an important scale. As is well known (see, *e.g.*, Ref. [39] for an analogous study in the dilepton context), larger energies increase the sensitivity of the exponential to temperature variations and thus will lead to a stronger weighting of earlier phases. To exhibit this interplay in a more realistic way, we include the weights from the QGP and hadronic spectral functions, $\mathrm{Im}\,\Pi_{\mathrm{EM}}$, in plotting the temperature-differential photon spectra for two representative transverse energies (see upper right and lower panel of Fig. 3); in other words, we use the full rate expression - the same for both evolution models - figuring in our comparisons to data in the following sections (recall that the AMY QGP rates (full LO result) [26] and the TRG hadronic rates [19] are nearly degenerate around T_{pc}, thus avoiding a "bias" for either phase). For low photon momenta (energies), $q_T = 0.5\,\mathrm{GeV}$, the "phase transition" peak observed in the four-volume is remarkably enhanced, but also the high-temperature part now exhibits significant emission strength. As expected, the high-temperature component increases further at larger momentum ($q_T = 2\,\mathrm{GeV}$), albeit not dramatically. A pronounced peak

around $T_{\rm pc}$ persists also for these kinematics.

This analysis clearly identifies the importance of the "pseudo-critical" regime, around $T_{\rm pc}$, for thermal photon radiation, as found in Ref. [9]. The macrophysics encoded in the underlying EoS plays an important role through a rapid change in entropy density over a rather small temperature window, possibly augmented by a reduction in the velocity of sound, $c_{\rm s}^2$, figuring into the hydro evolution (a pertinent slowing down has not been implemented into the fireball evolution). An equally important role is plaid by the microphysics, *i.e.*, relatively large hadronic emission rates, comparable to the QGP ones, in the transition region. Together with substantial flow-induced blue shifts, this led to generating a sizable photon v_2 in our previous fireball calculations [9]. These features can be recovered within hydrodynamic evolutions, *if* the collective flow is built up sufficiently fast, which can be realized via a modest initial radial-flow field and a compact initial-density profile. However, quantitative differences remain, which we further analyze in the following two sections by comparing the photon spectra from both approaches with each other and to direct photon data at RHIC and LHC.

3. Direct Photon Spectra at RHIC and LHC

All thermal photon spectra presented in this section are based on the same emission rates, from a complete LO calculation in a perturbative QGP [26] and hadronic many-body calculations supplemented with t-channel meson exchange reactions [19] as well as $\pi\pi$ and πK Bremsstrahlung [40]. We also note that short-lived (strong) resonance decays are usually not subtracted from the experimental spectra. To account for these "strong feeddown" photons (*e.g.*, $\Delta \to N\gamma$, etc.), we follow Refs. [41, 9] by running our evolution for an extra 1 fm/c after kinetic freezeout. Strictly speaking, as elaborated in Ref. [42], these final-state decays would have to be calculated with slightly modified kinematics compared to thermal processes (with an extra Lorentz-γ factor), but we neglect this difference in the present study. Ultimately, their contribution to the total direct-γ v_2 turns out to be rather modest (e.g., increasing it by typically 5-10% around $q_T = 2\,$GeV), and even less for the spectra.

3.1. Thermal Fireball

We start by updating the fireball calculations at RHIC, which in Ref. [9] where conducted with a first-order EoS (and a by now outdated chemical-freezeout temperature of $T_{\rm ch} = 180\,$MeV), by implementing the *latPHG* EoS of Ref. [28] with chemical freezeout at $T_{\rm ch} = 160\,$MeV. The resulting thermal spectra are compared to the results of Ref. [9] in Fig. 5 using the same total entropy. Since the partitioning of hadronic and QGP emission in the mixed phase of the first-order transition is now entirely assigned to the nonperturbative QGP phase, and due to a lower critical temperature in the *latPHG*, the QGP contribution significantly increases while the hadronic part decreases compared to the first-order scenario. This "reshuffling" by itself corroborates that the major portion of the thermal emission originates from around the phase transition region, independent of the details of the EoS. While the total (integrated) photon yield is not changed much (analogous to what has been found for low-mass dileptons [25]), the high-q_T part of the spectrum benefits from the increased temperature in the QGP close to $T_{\rm pc}$ and from the later chemical freezeout in the hadronic phase, which slows down the drop in temperature

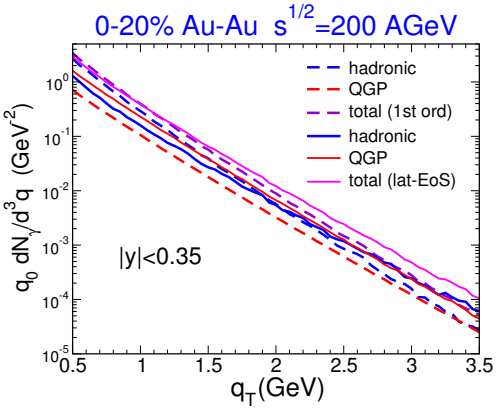

Figure 5: (Color online) Comparison of thermal photon spectra in Au+Au($\sqrt{s} = 0.2A$ TeV) collisions from an expanding fireball using either a first-order quasiparticle-QGP + HRG EoS with $T_c = T_{cm} = 180$ MeV [9] (dashed lines) or a cross-over lQCD + HRG EoS with $T_{pc} = 170$ MeV and $T_{ch} = 160$ MeV; red, blue and purple/pink lines represent QGP, hadronic and total contributions, respectively.

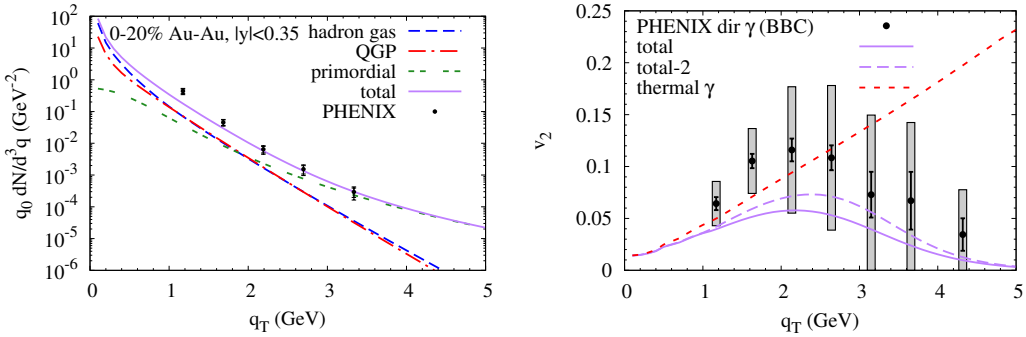

Figure 6: (Color online) Direct photon spectra (left panel) and elliptic flow (right panel) from the expanding fireball in 0-20% Au+Au($\sqrt{s} = 0.2\,A$TeV) collisions with updated total entropy using the *latPHG* EoS, compared to PHENIX data [15, 22]. In the left panel, blue dashed, red dashed-dotted, green short-dashed-dotted and purple solid lines correspond to hadronic, QGP and primordial contributions, and their sum ("total"), respectively. The primordial conribution is based on the PHENIX pp parameterization. In the right panel, the red short-dashed line is the combined thermal v_2; the purple solid and long-dashed lines are the total direct-photon v_2 using two different primordial contributions, either the PHENIX pp parameterization (as in the left panel) or an x_t-scaling ansatz (labeled "total-2"). Both primoridial contributions are assumed to carry vanishing v_2.

that arises in the presence of pion (and other effective) chemical potentials (for the inclusive yields, and at low q_T, the faster temperature drop is (over-) compensated by the fugacity factors).

As mentioned above, we have further updated our fireball calculations by a careful readjustment of the entropy when using *latPHG*, leading to a 20% decrease compared to Ref. [9]. With our nonlinear dependence of thermal photon production on the charged-particle multiplicity, $\propto N_{ch}^{x}$ with $x \simeq 1.5$ [19, 25] (larger at higher q_T), the thermal yields are somewhat reduced compared to our earlier results. The comparison to the PHENIX data for direct photons in Fig. 6 shows discrepancies at low q_T for both spectral yields and

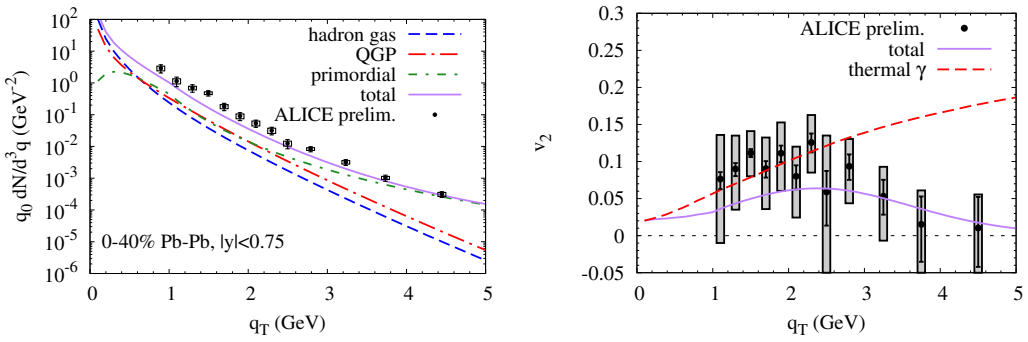

Figure 7: (Color online) Direct photon spectra (left panel) and elliptic flow (right panel) from the expanding fireball in 0-40% Pb+Pb($\sqrt{s} = 2.76\,A$TeV) collisions using *latPHG* EoS, compared to preliminary ALICE data [16, 23]. In the left panel, red, blue, green and purple lines represent QGP, hadronic and primordial contributions, as well as the total, respectively. In the right panel we show the combined thermal v_2 (red dashed line) and the total v_2 (purple solid line).

v_2, while for $q_T \geq 2\,$GeV the calculations are within the experimental errors. We illustrate uncertainties in the determination of the primordial photon component due to initial hard NN scatterings: on the one hand, we used a phenomenological parameterization by the PHENIX Collaboration of their pp data [15]; on the other hand, we used the x_t-scaling ansatz of Ref. [43], fitted to the high-q_T part of the PHENIX pp data with a K-factor of 2.5. The latter spectrum turns out to be somewhat smaller than the PHENIX parameterization at small q_T. This has rather little impact on the total q_T spectrum, but it affects the v_2 more significantly, inducing an increase of the total direct-photon v_2 of up to $\sim 25\%$ around $q_T \simeq 2.5\,$GeV. Further theoretical studies of the hard component are needed to better quantify this effect, *e.g.*, via a suppression of fragmentation photons or nuclear effects on the initial parton distribution functions.

Finally, we turn to LHC energies, where preliminary direct-photon data are available from ALICE for 0-40% central Pb+Pb($\sqrt{s} = 2.76\,A$TeV) collisions [16, 23]. We model these reactions with an average charged-particle multiplicity of $\mathrm{d}N_{\mathrm{ch}}/\mathrm{d}y = 1040$ over a rapidity interval of $|y| < 0.75$. For primordial photon production from binary NN collisions, we employ the x_t-scaling ansatz [43], fitted to the high-q_T ALICE photon spectra with a K-factor of 2. The description of the spectra and v_2 is at a comparable level as at RHIC, with indications for an underestimate in both observables in the regime where thermal radiation is most significant, cf. Fig. 7.

3.2. Ideal Hydrodynamics

The direct-photon results from the ideal-hydro tune with *latPHG* EoS and default emission rates at RHIC are displayed in Fig. 8. The QGP contribution to the q_T spectra agrees within ca. 30% with the fireball results, but the hadronic portion falls short by a larger margin, especially toward higher q_T. This is not unexpected as the lifetime of the hydro evolution in the hadronic phase is noticeably smaller, due to a faster cooling in the local rest frame of the ideal hydro cells (leading to smaller four-volumes, recall Fig. 3). In addition, the average temperature in the late stages is smaller in hydrodynamics than in the fireball (cf. upper left panel of Fig. 2), which leads to a reduction especially in the high-q_T region of the hadronic emission. Consequently, the hydro spectra and

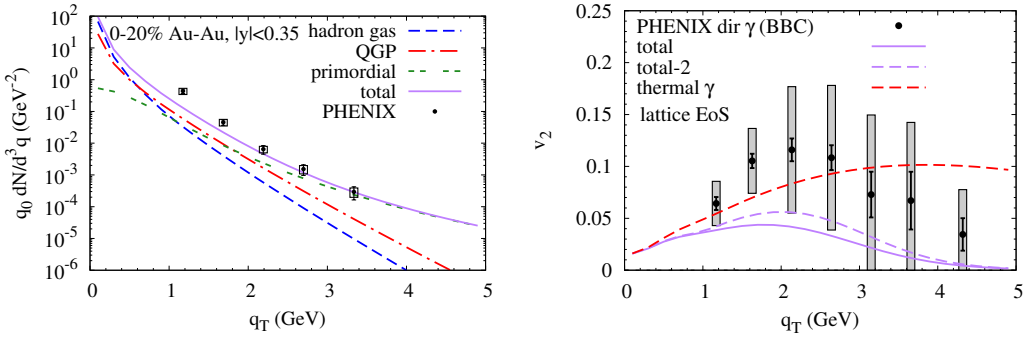

Figure 8: (Color online) Direct photon spectra (left panel) and v_2 (right panel) in Au+Au($\sqrt{s}$ = 0.2 ATeV) collisions using ideal hydrodynamics, compared to PHENIX data [15, 22]; line identifications as Fig. 6.

v_2 come out lower than for the fireball evolution; this increases the discrepancy with the PHENIX data for both observables, although not by much. Both evolution models result in an underestimate of the first two data points of the PHENIX spectra, and barely reach into the lower portions of the error bars of the v_2 data: the maximal v_2 reaches $\sim$ 4.4% for the hydrodynamic evolution, compared to $\sim$ 5.7% for the fireball, both when using the PHENIX pp baseline spectra (larger for the x_t scaling ansatz). However, our hydro results are well above other hydrodynamic calculations reported in the literature [8, 10, 44]. One difference lies in a faster build-up of the v_2, which essentially saturates when the system reaches the pseudo-critical region in the cooling process, for both fireball and hydro (cf. lower panel of Fig. 2). As mentioned above, this feature is essential in describing the spectra and v_2 of multistrange hadrons with an early kinetic freezeout close to the chemical freezeout temperature, and thus rather well motivated by hadron phenomenology (including the constituent-quark number scaling of v_2). In the hydrodynamic modeling this can be realized by initial conditions including a finite transverse flow at thermalization, together with a compact energy-density profile. Both features increase the transverse flow early on, which ultimately leads to an earlier saturation of v_2 (since the initial spatial anisotropy is converted faster into momentum space); it also increases the blue shift of the photons emitted from around $T_{\rm pc}$, which helps to build up the photon yield with large v_2 in the q_T = 2-3 GeV region. Another difference to existing hydro calculations is the larger rate in the hadronic phase, in particular the contributions associated with the photon point of the in-medium ρ spectral function, which includes sources from interactions involving baryons and antibaryons [41] and higher excited meson resonances [45].

Next, we turn to our hydro results at LHC, adopting a similar ansatz for the initial conditions as at RHIC, *i.e.*, with a finite transverse flow and compact entropy density profile. A factor of $\sim$ 2 underestimate of the preliminary photon spectra measured by ALICE in 0-40% Pb-Pb($\sqrt{s}$ = 2.76 ATeV) collisions is found for momenta below $q_T \simeq 2$ GeV, see left panel of Fig. 9. The calculated v_2 is not inconsistent with these data within the current experimental uncertainties, see right panel of Fig. 9. Although the hadronic component in the thermal spectra is again considerably smaller than in the fireball spectra, the relatively stronger QGP component in both calculations compared

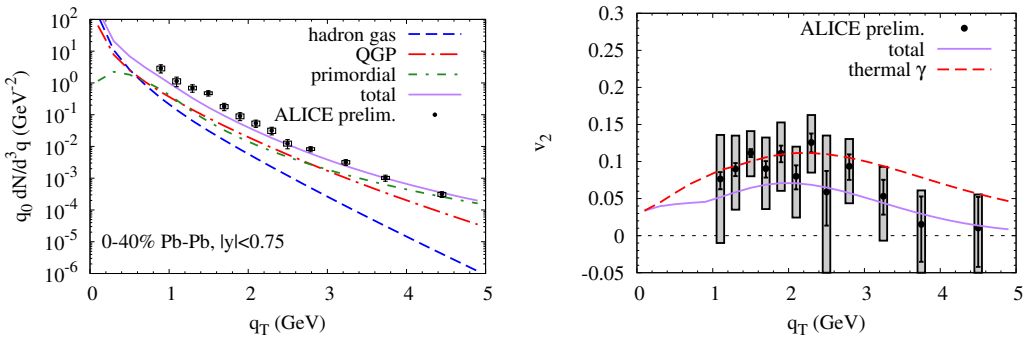

Figure 9: (Color online) Direct photon spectra (left panel) and v_2 (right panel) in 0-40% Pb+Pb($\sqrt{s} = 2.76\,A$TeV) collisions using ideal hydrodynamics, compared to preliminary ALICE data [16, 23]; line identifications as in Fig. 8.

to RHIC renders the overall impact of the hadronic emission less relevant. The QGP component from the hydro is now somewhat stronger than from the fireball (especially at high q_T), leading to closer agreement in the total photon spectra and v_2, and also with the data. Note that the v_2 of the thermal component at $q_T \gtrsim 3\,\mathrm{GeV}$ is significantly larger for the fireball than for the hydro (cf. dashed lines in the right panels of Figs. 7 and 9, respectively), due to the larger hadronic component in the former.

4. Discussion

The general trend of our results reported above for both fireball and hydrodynamic evolutions is an underestimate of both spectra and v_2 for both PHENIX and preliminary ALICE data for photon momenta $q_T \leq 3\,\mathrm{GeV}$, which is the region where the thermal radiation is expected to be most relevant. In the following, we will investigate possibilities how these deficits may be overcome. For simplicity, we concentrate on the hydrodynamic space-time evolution for these studies.

One option to increase thermal radiation in URHICs is a decrease of the thermalization time, τ_0, of the medium, as investigated, *e.g.*, in Refs. [46, 9, 47]. While the total yield generally increases above $q_T > 1\,\mathrm{GeV}$, its slope becomes harder and the total v_2 becomes smaller, both not favored by the data. This reiterates the need for a softer radiation source with larger v_2. In the following, we will stick to our default value of $\tau_0 = 0.6\,\mathrm{fm}/c$.

In Refs. [9, 48, 44] an enhancement of the photon emission rates in the pseudo-critical region, beyond the default rates used above, has been conjectured. This may not be unexpected, from a theoretical point of view. On the QGP side, the AMY rates are based on perturbative parton rescattering, which in other contexts tends to fall short in producing sufficient interaction strength, *e.g.*, in both phenomenology and lattice calculations of η/s or the heavy-quark diffusion coefficient [49, 50]. Especially close to the hadronization transition, confining interactions are expected to play an important role (as, *e.g.*, borne out of lattice calculations for the heavy-quark free energies [51]). An increase in partonic scattering rates is a natural mechanism to also increase photon radiation (see, *e.g.*, Ref. [52]), which is quite different from a perturbative scenario with

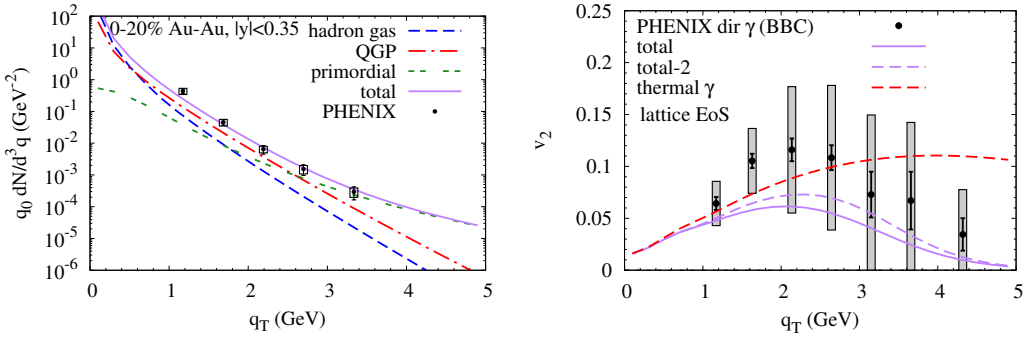

Figure 10: (Color online) Direct photon spectra (left panel) and v_2 (right panel) from hydrodynamics at RHIC when introducing a "pseudo-critical" enhancement of QGP and hadronic rates around $T_{\rm pc}$, compared to PHENIX data [15, 22]; line identifications as Fig. 6.

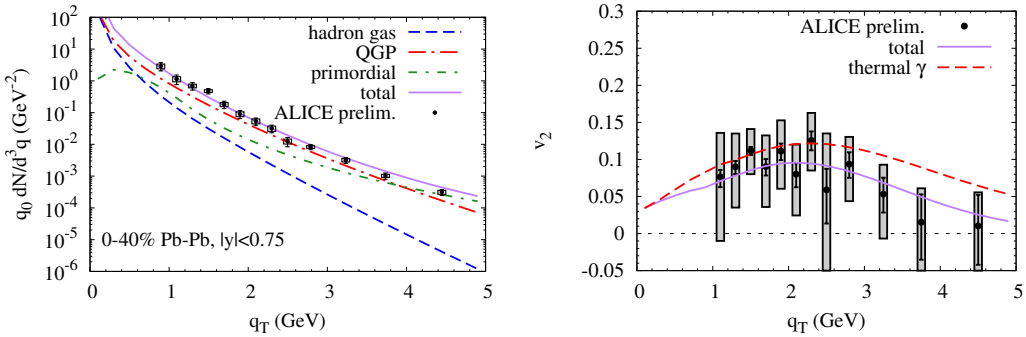

Figure 11: (Color online) Direct photon spectra (left panel) and v_2 (right panel) at LHC with enhanced photon rates around $T_{\rm pc}$, compared to preliminary ALICE data [16, 23].

weakly interacting quasi-particles. On the hadronic side, an enhancement of the current rates is conceivable as well, since the TRG rates (including contributions from the in-medium ρ spectral function) may not exhaust all relevant reaction channels in hadronic resonance matter; investigations to identify and calculate possibly important channels not considered thus far are in progress [53] (we note in passing that hadronic Bremsstrahlung is an unlikely candidate since its spectrum tends to be too soft [40]). To mimic a "pseudo-critical" enhancement of our default rates, we increase the latter by a baseline factor of 2, further amplified up to a maximum factor of 3 at $T_{\rm pc} = 170\,$MeV, linearly ramped up from $T = 140\,$MeV and down until $T = 200\,$MeV again. The results are encouraging (cf. Figs. 10 and 11): the description of both PHENIX and preliminary ALICE spectra and v_2 improves significantly. The calculated v_2 at RHIC still tends to only reach into the lower portions of the experimental errors, but we recall that larger hadronic contributions, as suggested by the fireball calculations, would help to increase it further.

Let us briefly expand on a speculation raised in Ref. [9], that there might be an hitherto undetermined uncertainty in the subtraction of the radiative $\omega \to \pi^0\gamma$ decays, since the latter have not been explicitly measured in the low-q_T region in the Au-Au environment. For this purpose, and to obtain an absolute upper estimate, we simply add to our thermal spectra (calculated with the amplified rates) the photon contribution from

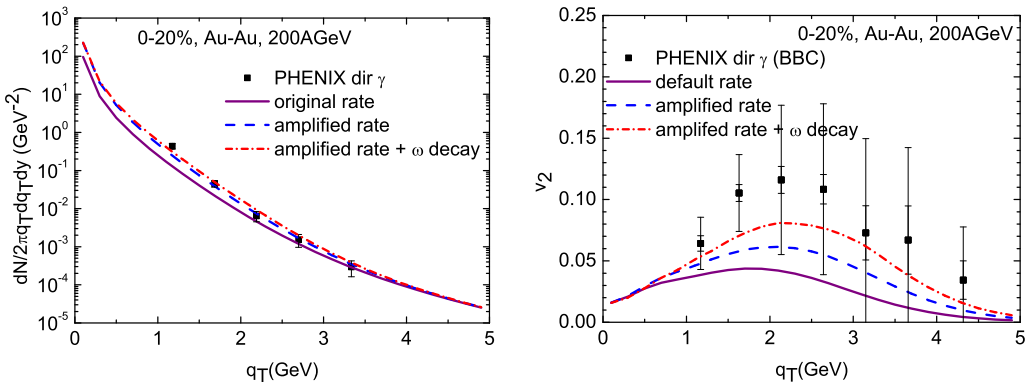

Figure 12: (Color online) Direct photon spectra (left panel) and v_2 (right panel) from hydrodynamics at RHIC when adding $\omega \to \pi^0 + \gamma$ decays at thermal freezeout to the scenario with enhanced rates (dash-dotted line), compared to the enhanced-rate (dashed line) and default-rate (solid line) scenarios, as well as the PHENIX data [15, 22]; all calculations use the PHENIX pp baseline for the primordial component.

final-state ω decays based on our hydro ω spectra at thermal freezeout (as a three-pion or $\rho\pi$ resonance, the ω receives a pion fugacity factor to the third power). The result of this exercise is shown in Fig. 12, illustrating an appreciable effect on both spectra and v_2 which would still be significant if reduced by a factor of 2.

Finally, we conduct a schematic study of the effect of quark undersaturation in the early (Q)GP phases, as expected from gluon saturation models [54]. Similar to earlier calculations for thermal EM emission [55, 56, 24], we find the gluon Compton process, $gq \to q\gamma$, to still contribute appreciably (and with a harder slope than in a chemically equilibrated QGP at the same total entropy), unless the $q\bar{q}$ undersaturation is strong enough to largely suppress the early thermal yield altogether. This suppression would have to be made up by an even larger enhancement in the later phases compared to what we assumed above.

5. Summary and Conclusions

In this paper we have studied the properties of thermal photon radiation at collider energies, in an attempt to better understand recent measurements of direct photon spectra and their elliptic flow. Using QGP and hadronic thermal emission rates as available from the literature, we first focused on a detailed comparison of the space-time evolution as given by a blast-wave type fireball and ideal hydrodynamics. Both were based on the same equation of state and fits to the same set of hadron data using the concept of sequential freeze-out for multistrange and light hadrons. The relevance of this concept for photon radiation lies in a rather early saturation of v_2 and larger blue shifts by the time the expanding system reaches the phase transition region (in the hydro model, this can be realized by compact initial conditions with non-zero radial flow). We have found that the emission characteristics of the QGP part agree rather well between hydro and fireball, while the latter leads to significantly larger photon radiation in the hadronic phase, especially toward higher q_T. We traced this back to a slower cooling with larger

average temperatures and radial flow in the fireball, which, at least in part, is due to a continuous freezeout in hydrodynamics leading to an appreciable reduction of the "active" matter cells in the later stages of the evolution. Both evolution models clearly identify the transition region around $T_{\rm pc} \simeq 170\,{\rm MeV}$ as a key source of thermal photon emission. After the addition of primordial photons extrapolated from pp collisions, both hydro and fireball results tend to be somewhat (although not dramatically) below the measured spectra and v_2 in Au-Au and Pb-Pb collisions at RHIC and LHC, with a preference for the fireball due to its larger hadronic contribution. We then shifted our focus to the microscopic emission rates. We argued that an enhancement of the currently employed emission rates is plausible, especially in the pseudo-critical region where the medium is expected to be most strongly coupled. Upon amplifying our default rates by a baseline factor of 2, reaching up to 3 around $T_{\rm pc} \pm 30\,{\rm MeV}$, we found that the photon results from the hydro model come rather close to the experimental spectra and v_2 within current uncertainties. The additional hadronic contributions suggested by the fireball model would further improve the situation. Microscopic calculations of photon rates to search for additional sources not considered thus far are underway.

Acknowledgments.– We thank C. Gale and R.J. Fries for discussions, and gratefully acknowledge fruitful exchanges at the EMMI RRTF workshop on "Direct-photon flow puzzle" organized by K. Reygers and J. Stachel. This work has been supported by the U.S. National Science Foundation through grants PHY-0969394 and PHY-1306359, by the Humboldt Foundation, by NSFC grant 11305089, by the German Federal Ministry of Education and Research (BMBF Förderkennzeichen 05P12RFFTS), and by the Hessian initiative for excellence (LOEWE) through the Helmholtz International Center for FAIR (HIC for FAIR).

References

[1] J. Alam, S. Sarkar, P. Roy, T. Hatsuda and B. Sinha, Annals Phys. **286**, 159 (2001).
[2] T. Peitzmann and M.H. Thoma, Phys. Rep. **364**, 175 (2002).
[3] F. Arleo *et al.*, arXiv:hep-ph/0311131.
[4] R. Rapp, J. Wambach and H. van Hees, in *Relativistic Heavy-Ion Physics*, edited by R. Stock and Landolt Börnstein (Springer), New Series **I/23A**, 4-1 (2010); [arXiv:0901.3289[hep-ph]].
[5] C. Gale, in *Relativistic Heavy-Ion Physics*, edited by R. Stock and Landolt Börnstein (Springer), New Series **I/23A**, 6-3 (2010); arXiv:0904.2184 [hep-ph].
[6] R. Chatterjee, E.S. Frodermann, U.W. Heinz and D.K. Srivastava, Phys. Rev. Lett. **96**, 202302 (2006).
[7] F.-M. Liu, T. Hirano, K. Werner and Y. Zhu, Phys. Rev. C **80**, 034905 (2009).
[8] H. Holopainen, S. Räsänen and K.J. Eskola, Phys. Rev. C **84**, 064903 (2011).
[9] H. van Hees, C. Gale and R. Rapp, Phys. Rev. C **84**, 054906 (2011).
[10] M. Dion, J.-F. Paquet, B. Schenke, C. Young, S. Jeon and C. Gale, Phys. Rev. C **84**, 064901 (2011).
[11] P. Mohanty, V. Roy, S. Ghosh, S.K. Das, B. Mohanty, S. Sarkar, J. -e Alam and A.K. Chaudhuri, Phys. Rev. C **85**, 031903 (2012).
[12] C. Shen, U.W. Heinz, J.-F. Paquet, I. Kozlov and C. Gale, arXiv:1308.2111 [nucl-th].
[13] O. Linnyk, W. Cassing and E. Bratkovskaya, Phys. Rev. C **89**, 034908 (2014).
[14] M.M. Aggarwal et al. [WA98 Collaboration], Phys. Rev. Lett. **85**, 3595 (2000).
[15] A. Adare *et al.* [PHENIX Collaboration], Phys. Rev. Lett. **104**, 132301 (2010).
[16] M. Wilde [ALICE Collaboration], Nucl. Phys. A **904-905**, 573c (2013).
[17] D.K. Srivastava and B. Sinha, Phys. Rev. C **64**, 034902 (2001).
[18] P. Huovinen, P.V. Ruuskanen and S.S. Räsänen, Phys. Lett. B **535**, 109 (2002).
[19] S. Turbide, R. Rapp and C. Gale, Phys. Rev. C **69**, 014903 (2004).
[20] P. Mohanty, J.K. Nayak, J.-e Alam and S.K. Das, Phys. Rev. C **82**, 034901 (2010).
[21] B. Bauchle and M. Bleicher, PoS BORMIO **2010**, 062 (2010).

[22] A. Adare *et al.* [PHENIX Collaboration], Phys. Rev. Lett. **109**, 122302 (2012).
[23] D. Lohner *et al.* [ALICE Collaboration], J. Phys. Conf. Ser. **446**, 012028 (2013).
[24] R. Rapp, Phys. Rev. C **63**, 054907 (2001).
[25] R. Rapp, Adv. High Energy Phys. **2013**, 148253 (2013).
[26] P.B. Arnold, G.D. Moore and L.G. Yaffe, JHEP **0112**, 009 (2001).
[27] M. He, R.J. Fries and R. Rapp, Phys. Rev. C **82**, 034907 (2010).
[28] M. He, R.J. Fries and R. Rapp, Phys. Rev. C **85**, 044911 (2012).
[29] A. Andronic, P. Braun-Munzinger and J. Stachel, Nucl. Phys. A **772**, 167 (2006).
[30] J. Stachel, A. Andronic, P. Braun-Munzinger and K. Redlich, arXiv:1311.4662 [nucl-th].
[31] R. Rapp, Phys. Rev. C **66**, 017901 (2002).
[32] P.F. Kolb and U.W. Heinz, In R. C. Hwa (ed.) et al.: Quark gluon plasma, 634, [nucl-th/0305084].
[33] B.I. Abelev *et al.* [STAR Collaboration], Phys. Rev. Lett. **99**, 112301 (2007).
[34] S.S. Adler *et al.* [PHENIX Collaboration], Phys. Rev. Lett. **91**, 182301 (2003).
[35] S.S. Adler *et al.* [PHENIX Collaboration], Phys. Rev. C **69**, 034909 (2004).
[36] J. Adams *et al.* [STAR Collaboration], Phys. Rev. Lett. **92**, 112301 (2004).
[37] S. Pratt, Phys. Rev. Lett. **102** (2009) 232301.
[38] F. Grassi, Braz. J. Phys. **35**, 52 (2005).
[39] R. Rapp, Acta Phys. Polon. B **42**, 2823 (2011).
[40] W. Liu and R. Rapp, Nucl. Phys. A **796**, 101 (2007).
[41] R. Rapp and J. Wambach, Eur. Phys. J. **A6**, 415 (1999).
[42] H. van Hees and R. Rapp, Nucl. Phys. A **806**, 339 (2008).
[43] D.K. Srivastava, Eur. Phys. J. C **22**, 129 (2001).
[44] C. Shen, U.W. Heinz, J.-F. Paquet and C. Gale, arXiv:1308.2440 [nucl-th].
[45] R. Rapp and C. Gale, Phys. Rev. C **60**, 024903 (1999).
[46] R. Chatterjee and D.K. Srivastava, Phys. Rev. C **79**, 021901 (2009).
[47] R. Chatterjee, H. Holopainen, T. Renk and K.J. Eskola, Phys. Rev. C **85**, 064910 (2012).
[48] R. Rapp, PoS CPOD **2013**, 008 (2013).
[49] T. Schäfer and D. Teaney, Rept. Prog. Phys. **72**, 126001 (2009).
[50] R. Rapp and H. van Hees, R. C. Hwa, X.-N. Wang (Ed.) Quark Gluon Plasma 4, World Scientific, 111 (2010).
[51] O. Kaczmarek and F. Zantow, Phys. Rev. D **71**, 114510 (2005).
[52] V.V. Goloviznin, A.M. Snigirev and G.M. Zinovjev, JETP Lett. **98** (2013) 61.
[53] N. Holt, P. Hohler and R. Rapp, work in progress.
[54] L. McLerran and B. Schenke, arXiv:1403.7462 [hep-ph].
[55] M. Strickland, Phys. Lett. B **331**, 245 (1994).
[56] D.K. Srivastava, M.G. Mustafa and B. Müller, Phys. Rev. C **56**, 1064 (1997).